Nanoscale

Accepted Manuscript

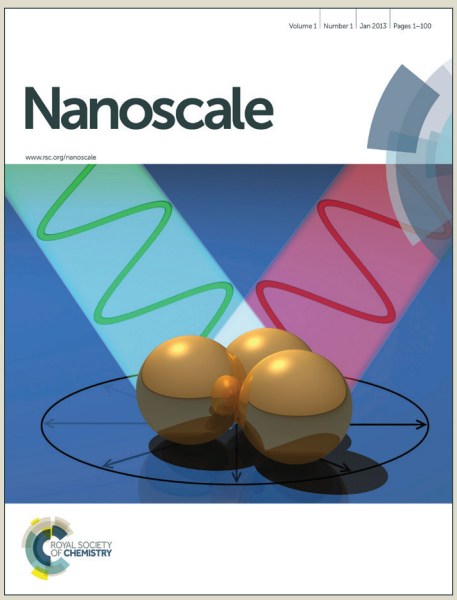

ROYAL SOCIETY OF CHEMISTRY

www.rsc.org/nanoscale

Solvent-like ligand-coated ultrasmall cadmium selenide nanocrystals: Strong electronic coupling in a self-organized assembly

Katie N. Lawrence,[a] Merrell A. Johnson,[b] Sukanta Dolai,[a] Amar Kumbhar,[c] and Rajesh Sardar,[*a,d]

[a]Department of Chemistry and Chemical Biology, Indiana University-Purdue University Indianapolis, 402 N. Blackford Street, Indianapolis, Indiana 46202, United States.

[b]Department of Physics, Indiana University-Purdue University Indianapolis, 402 N. Blackford Street, Indianapolis, Indiana 46202, United States.

[c]Chapel Hill Analytical and Nanofabrication Laboratory, University of North Carolina, Chapel Hill, North Carolina, 27599, United States.

[d]Integrated Nanosystems Development Institute, Indiana University-Purdue University Indianapolis, 402 N. Blackford Street, Indianapolis, Indiana 46202, United States.

[*]E-mail: rsardar@iupui.edu

ABSTRACT

Strong inter-nanocrystal electronic coupling is a prerequisite for delocalization of exciton wave functions and high conductivity. We report 170 meV electronic coupling energy of short chain poly(ethylene glycol) thiolate-coated ultrasmall (<2.5 nm in diameter) CdSe semiconductor nanocrystals (SNCs) in solution. Cryo-transmission electron microscopy analysis showed the formation of a *pearl-necklace* assembly of nanocrystals in solution with regular inter-nanocrystal spacing. The electronic coupling was studied as a function of CdSe nanocrystal size where the smallest nanocrystals exhibited the largest coupling energy. The electronic coupling in spin-cast thin-film (<200 nm in thickness) of poly(ethylene glycol) thiolate-coated CdSe SNCs was studied as a function of annealing temperature, where an unprecedentedly large, ~400 meV coupling energy was observed for 1.6 nm diameter SNCs, which were coated with a thin layer of poly(ethylene glycol) thiolates. Small-angle X-ray scattering measurements showed that CdSe SNCs maintained an order array inside the films. The strong electronic coupling of SNCs in a self-organized film could facilitate the large-scale production of highly efficient electronic materials for advanced optoelectronic device application.

TOC Graphic

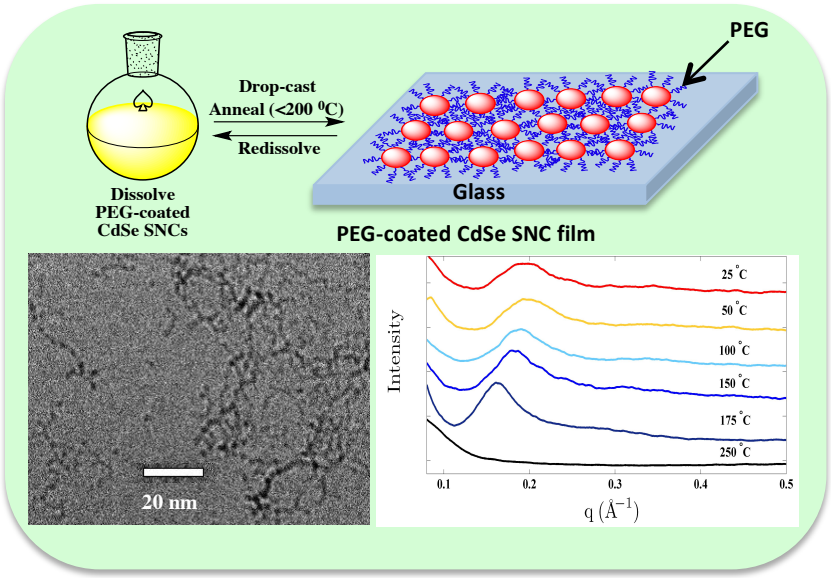

One sentence text: Strong inter-nanocrystal electronic coupling is demonstrated between short chain poly(ethylene glycol) thiolate-coated ultrasmall (<2.5 nm in diameter) CdSe semiconductor nanocrystals both in the colloidal state and as dry films on solid surfaces.

INTRODUCTION

The electronic and photophysical properties of semiconductor nanocrystals (SNCs) are substantially controlled by their surface ligand chemistry.[1-6] The surface passivating ligands are generally introduced during the SNC synthesis to enhance solution dispersibility, stability, and to expand their potential application in light-emitting diodes,[7-10] photodetectors,[11, 12] field-effect transistors,[13, 14] and photovoltaics.[15, 16] However, commonly used long-chain aliphatic ligands are electrically insulating, which leads to poor carrier mobilities and conductivities and therefore can have deleterious effects on thin-film-based optoelectronic devices. The conductivity in SNC films can be improved by increasing inter-SNC electronic coupling by reducing the thickness of the insulating ligand shell because when two SNCs are brought into close vicinity, their exciton (bound electron-hole pair) wave functions can expand beyond the SNC boundary and participate in electronic coupling. Use of this property of the SNC films would open a new frontier of scientific research by enabling the preparation of "artificial solids" with unprecedentedly high conductivity.[17]

A number of methods have been developed to enhance the electronic coupling between SNCs in colloidal dispersion and/or solid films by exchanging the native bulky, hydrocarbon ligands with small organic ligands,[18-21] inorganic ions,[22-28] and metal chalcogenide complexes.[13, 29-31] The solid phase ligand exchange reaction can cause a dramatic structural rearrangement of SNCs, which results in the appearance of cracks and voids in the solid films or irreversible aggregation of SNCs inside the films.[19, 32] In contrast, a solution phase exchange reaction would enable preservation of the solution dispersibility, which allows for better solution processing for more efficient film preparation. Various ligands such as chloride,[22] thiocyanate,[25] sulfide,[26-28] metal chalcogenide complexes,[13, 29-31] tetrafluoroborate,[23, 24] hydrazine,[14, 32] and pyridine[19] have

most commonly been used to perform solution phase exchange reactions. However, these newly formed ligand-coated SNCs do not show any electronic coupling in solution, which would present as a red-shift of the excitonic peaks in the absorption spectrum.[33-35] Additionally, ligand exchange reactions with these small ligand molecules often create trap states and recombination sites that nullify the advantage of strong electronic coupling in the film.[27, 29] Moreover, SNCs coated with either small molecules or various ions are unstable, susceptible to undergoing fast oxidation even at ambient conditions,[19] and only soluble in high boiling solvents,[13, 19, 25, 28, 31, 36] all of which makes processing during device fabrication very challenging.

The above-mentioned difficulties can be avoided through a solution phase exchange reaction with moderately long chain ligands where the SNCs will not only retain their solution dispersibility but also enable facile thin-film preparation with strong electronic coupling. Short chain length organic molecules such as 1,2-ethanedithiol,[18] 1,6-hexanedithiol,[37] and mercaptobenzoic acid[38] were used to replace the original insulating ligands and the resulting ligand-coated SNCs displayed electronic coupling in solution. However, these ligand-coated large SNCs (>3.0 nm in diameter) displayed weak electronic coupling.[18, 37, 38] Importantly, it was also shown that coupling increases as the size of the nanocrystals decreases.[33, 37] Therefore, we could expect that ultrasmall SNCs with <3.0 nm in diameter would display strong electronic coupling in solution through ordered arrays and/or reduction of inter-SNC distance with appropriate selection of surface passivating ligands. Moreover, such ligand choice may allow SNCs to maintain good solution stability and dispersibility properties for the preparation of thin-films with long-range electronic coupling, additionally eliminating the need for extra foreign metal layer deposition.[27]

This article describes the investigation of electronic coupling of poly (ethylene glycol) (PEG)-thiolate-coated CdSe SNCs both in solution and as thin films by measuring excitonic peak energy using UV-vis absorption spectroscopy. The "*solvent-like"* character of PEGs, along with their low hydrodynamic radii,[39] allow strong inter-SNC interaction through entanglement of excitonic wavefunctions. Through systematic variation of the glycol unit (n = 4 to 150) in PEG chains, we have shown that the inter-SNC spacing was very important. We observed up to an ~170 meV change in coupling energy in solution. This is the highest value reported in the literature in the case of colloidal SNCs. The solution-phase organization of PEG-thiolate-coated SNCs was further investigated with Cryo-transmission electron microscopy (TEM), which showed formation of *"pearl-necklace"* assemblies. The SNC size effects in electronic coupling were also investigated. Finally, we explored the electronic coupling of SNCs in spin-casted thin-films on solid surfaces as a function of annealing temperature. An ~400 meV decrease in excitonic peak energy was observed for PEG_6-thiolate-coated CdSe SNCs film upon annealing at 175 ^{o}C. Structural properties of thin-films were characterized by small-angle X-ray scattering (SAXS) to unravel the strong electronic coupling. Precise manipulation of electronic interactions due to delocalization of strongly confined excitons of ultrasmall SCNs, which are also capable of donating and accepting multiple charges, PEG-thiolate-coated SNCs can be considered as ionically conductive *hybrid redox polyethers*[40] with potential for future applications in solid-state device fabrication.

EXPERIMENTAL SECTION

Materials. $CdSO_4$•8/3 H_2O (>99%), selenium metal (99.99%), triphenylphosphine (>99%) different chain length poly(ethylene glycol) methyl ethers (PEG_n, n = glycol unit = 6-150), p-

toluene sulfonyl chloride (>99%), thiourea (>99%), anhydrous acetonitrile (CH_3CN, >99.8%), hexanes (>99%), ethanol (98.5%), methanol (98.5%), chloroform (>99%), oleylamine (OLA, >70%), 1-hexanethiol (>95%), toluene (>99%), and dichloromethane (CH_2Cl_2, >99%) were purchased from Aldrich and used without further purification. Organic solvents were purged with nitrogen for 30 min prior to use. Glass coverslips were purchased from Electron Microscopy Sciences. All water was purified using a Thermo Scientific Barnstead Nanopure system. A 0.25 M aqueous solution of Na_2SeSO_3 was prepared for CdSe SNCs synthesis. PEG_n-thiols were synthesized according to literature procedure.[41] PEG_n-thiolate-coated CdSe SNCs were synthesized using our published procedure with slight modification.[42] A detailed procedure is provided in the Electronic Supplementary File (ESI). OLA-coated CdSe SNCs (1.6-2.5 nm diameter) were synthesized according to our published procedure (see ESI).[43]

Spectroscopy, Microscopy, and Spectrometry Measurements. UV-vis absorption spectra were collected using a Varian Cary 50 UV-vis spectrophotometer over a range of 300-800 nm. Prior to sample measurements, the baseline was corrected with pure solvent. For HRTEM analysis samples were prepared inside a glovebox by placing a drop of dissolved CdSe SNCs in CH_3CN onto a lacey carbon-coated copper grid (Electron Microscopy Science). Cryo-TEM analysis was conducted using a JEOL-3200FS-JEM instrument at 200 kV beam energy. The aqueous solution of the samples was frozen using liquid nitrogen. SEM micrographs were acquired using a Hitachi S-4700 FESEM at 20 kV. Any excess solution was removed by wicking with a Kimwipe to avoid particle aggregation. ^{1}H NMR was recorded on a Bruker AVANCE III 500 instrument at 500 MHz frequency. Approximately 5 mg of sample was dissolved in 0.6 mL of CD_2Cl_2 at room temperature and a minimum of 1000 scans were collected. Matrix-assisted laser desorption

ionization time of flight mass spectrometry (MALDI-TOF MS) measurements were performed using a Bruker Autoflex equipped with a nitrogen laser. The matrix consisted of 2-[(2E)-3-(4-tert-butylphenyl)-2-methylprop-2-enylidene]malononitrile (DCTB). CdSe SNCs were dissolved in DCM and mixed with DCTB in THF (20 nM). An approximately 5 μL of the matrix solution was then mixed with 1 μL of sample, vortexed, and 2 μL of this mixture was applied to the target and air-dried.

Ligand Exchange Reaction. Purified OLA-capped CdSe SNCs (1.6-2.5 nm diameter) were dissolved in 5.0 mL of nitrogen-purged chloroform to obtain a concentration of 0.25 mM. A 0.3 g of PEG_6-SH was added to OLA-coated CdSe SNCs at room temperature and stirred (~6 h) until a stable band-edge excitonic peak was obtained. The solution was then brought to dryness and the solid was redissolved in a minimum amount of CH_2Cl_2 and precipitated with hexane. The resulting solid was collected by centrifugation. The precipitation step was performed once more to remove excess PEG_6-SH. The similar ligand exchange reactions were performed for other PEG_n-SH. The soluble PEG_n-thiol-coated CdSe SNCs were characterized by ^{1}H NMR, MALDI-TOF-MS, and PL analyses to determine the structural properties.

Film Preparation. Glass coverslips (2.0 x 2.0 cm^2) were cleaned using piranha solution (7:3 volume ratio of H_2SO_4:30% H_2O_2) for 30 min. (Warning: Piranha solution is very corrosive and must be handled with extreme care. It violently reacts with organic materials). The coverslips were rinsed with nanopure water and sonicated in 5:1:1 volume ratio of H_2O:NH_4OH:30% H_2O_2 solution for 1 h. The coverslips were then rinsed with copious amount of water. The coverslips were cut into 2.0 cm x 1.0 cm area and dried at 150 ^oC in a vacuum oven for 30 min and allowed

to cool to room temperature prior to film preparation. A 100 μL (0.25 mM) PEG_6-thiolate-coated CdSe SNC solution in CH_3CN was spin-cast onto coverslips (10 s @ 800 rpm and then 15 s @1400 rpm), yielding a film of 350-400 nm thickness. The coverslips were then transferred to a pre-heated vacuum oven (40 to 250 ^{0}C) and allowed to anneal for 10 min. The film was then brought to room temperature under nitrogen atmosphere before any further spectroscopy and microscopy characterization.

RESULTS AND DISCUSSION

Recently, we reported an efficient synthetic method of preparation of PEG_n -thiolate-protected ultrasmall CdSe SNCs (<2.0 nm in diameter) and their potential application as inorganic fluorophores for *in vitro* cell imaging.[42] The SNCs were readily soluble in a diverse range of nonpolar and polar organic solvents and maintained long-term colloidal stability. The transmission electronic microscopy (TEM) analysis showed that both PEG_6- and PEG_{18}-thiolate-coated CdSe SNCs were 1.6 nm in diameter but their first excitonic peaks were 429 and 424 nm, respectively. Their sharp exciton peaks also resembled "magic-sized" SNCs.[43-46] The hydrodynamic radii of PEG_6-thiolate-coated CdSe SNCs, determined from dynamic light scattering (DLS) technique, indicated more than two SNCs were connected together in solution. The DLS measurements also suggested that the PEG_n chains were not fully extended in the solution. Based on these analyses we hypothesized that the 5 nm (30 meV) difference in the excitonic peak position between PEG_6- and PEG_{18}-thiolate-coated CdSe SNCs was controlled by differences in the inter-SNC distance, resulting in better electronic coupling. In order to prove our hypothesis, 1.6 nm diameter CdSe SNCs were synthesized using various chain length PEG_n-thiolates as capping ligands (n = 4, 60, and 150).

PEG-Chain Length Dependent Inter-SNC Coupling. Various PEG_n-thiolate-coated CdSe SNCs were synthesized according to our previously published procedure [42] and a detailed protocol is provided in the experimental section. Fig. 1A illustrates the UV-vis absorption spectra of different chain length PEG-thiolate-coated CdSe SNCs dissolved in CH_2Cl_2. The band-edge excitonic peak was 5 nm blue-shifted as glycol units in the PEG chain was increased from four to six. By increasing glycol units to 150, a total 20 nm blue shift of the excitonic peak was observed. Therefore a total 25 nm (170 meV) difference in peak position was detected between PEG_4- and PEG_{150}-thiolate-coated CdSe SNCs. We believe this blue-shift in the first excitonic peak is due to inter-SNC electronic coupling.

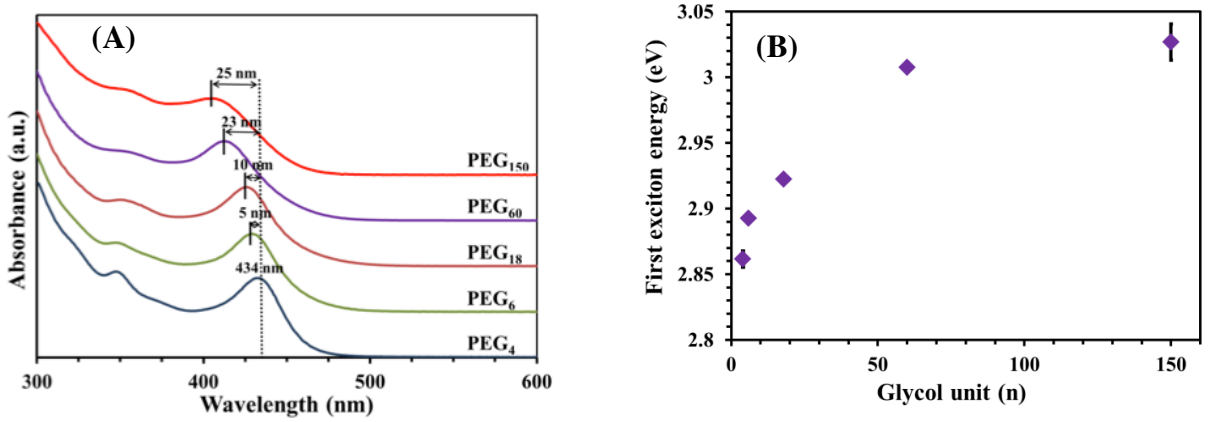

Fig. 1 (A) Room temperature UV-visible absorption spectra of purified samples of different chain length PEG_n-thiolate-coated CdSe SNCs in CH_2Cl_2. The HRTEM analysis demonstrated that the average size for each-type of PEG_n-thiolate-coated CdSe SNCs were 1.6 nm. The blue shifting of the band-gap excitonic peak position from PEG_4 to PEG_{150} suggested inter-SNC electronic coupling. (B) Excitonic peak energy of different chain length PEG_n-thiolate-coated CdSe SNCs. An ~170 meV difference between first exciton energy of PEG_4 and PEG_{150} was observed in solution, which is defined as coupling energy.

Fig. 1B shows the position of the first excitonic energy as a function of glycol unit. We assume no apparent inter-SNC electronic coupling has taken place in solution for PEG_{150}-thiolate-coated CdSe SNCs because the thick dielectric shell of PEG_{150}-thiolate is a good insulator. Therefore, we hypothesize that the change in coupling energy that is observed (up to

170 meV) was solely due to electronic coupling, which was controlled by the inter-SNC spacing. To the best of our knowledge, this is the highest value reported in literature for an electronic coupling of any type of SNCs in solution.[37, 38] In order for the SNCs to participate in strong electronic coupling, their electron and/or hole wave functions are required to expand outside the boundary of the isolated SNC, overlap, and entangle to form a delocalized state which reduces the excitonic band gap (red-shift of the peak position). It is known that the delocalization kinetic energy of the excitons is higher in strongly confined ultrasmall SNCs than intermediate or weakly confined larger SNCs.[47, 48] Therefore, at the ultrasmall size regime, the quantum-confined electron and/or hole wave functions could fill the entire SNC core volume more effectively and delocalize to the adjacent SNCs. This behavior is in contrast to SNCs with >3.0 nm diameter where wave functions are more localized inside the inorganic core,[49] and for which negligible electronic coupling has been reported in the literature even though they were coated with small molecules or ions.[13, 18, 25, 26, 31, 33, 37, 38] To better understand the strength of electronic coupling in solution, we also investigated the dependence of coupling energy as a function of CdSe SNCs size (<3.0 nm) as discussed later in this article.

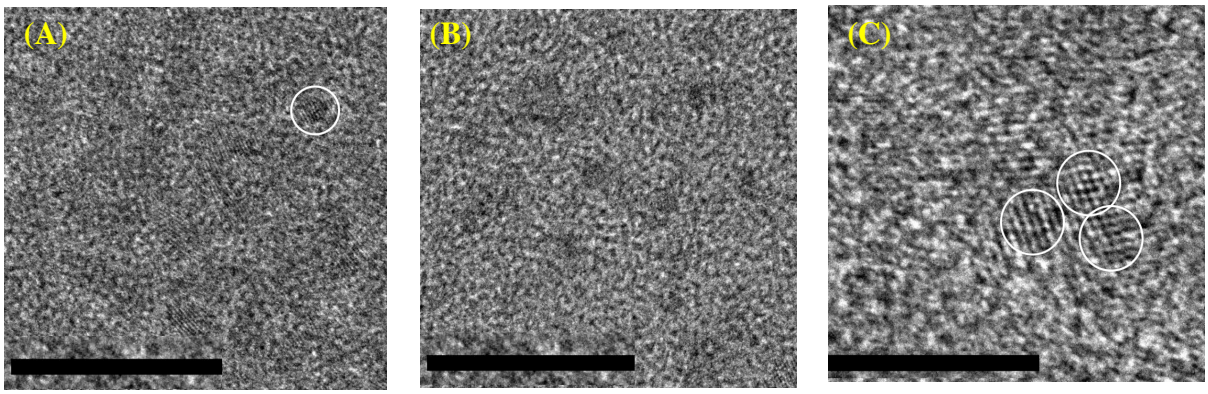

Fig. 2 HRTEM images of PEG_4- (A) and PEG_{150}- (B) thiolate-coated CdSe SNCs. The circle in (A) shows an isolated SNC with diameter ~1.6 nm. The scale bars are 10 nm. (C) Selected area HRTEM image of PEG_4-thiolate-coated CdSe SNCs demonstrating three individual SNCs were self-assembled. The scale bar is 5 nm.

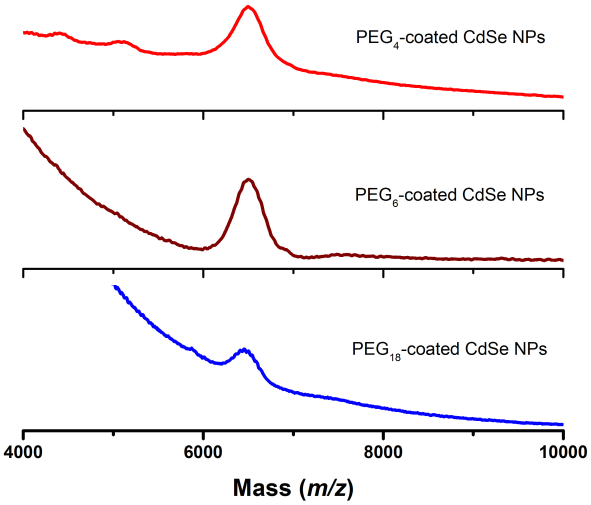

Fig. 3 MALDI-TOF-MS spectra of PEG_4- (red) PEG_6- (brown), and PEG_{18}- (blue) thiolate-coated CdSe SNCs. CdSe SNCs were dissolved in CH_2Cl_2 and mixed with DCTB matrix in THF with 1:1000 SNCs : matrix ratio.

Besides inter-SNC electronic coupling, which controls the excitonic peak position for different PEG_n-thiolate-coated CdSe SNCs, other parameters such as SNC core diameter and variable dielectric constant of the PEG-thiolate shell could potentially modulate the peak position. We investigated the potential contribution of these parameters to the dramatic shift of excitonic peak of CdSe SNCs in solution. First, different PEG_n-thiolate-coated CdSe SNCs were analyzed by high-resolution TEM (HRTEM) to determine the core diameter as shown in Fig. 2. In most cases we observed aggregation on the TEM grid (because of the drying process), but individual SNCs of both PEG_4- and PEG_{150}-thiolate coating were 1.6 ± 0.2 nm in diameter, which is in agreement with the values we determined previously for either PEG_6- or PEG_{18}-thiolate-coated CdSe SNCs.[42] Interestingly, PEG_4-thiolate-coated CdSe SNCs were present in aggregated states consisting averagely of three to four individual SNC (Fig. 2C) whereas PEG_{150}-thiolate-coated CdSe SNCs were present as isolated SNCs. Precise determination of the size of

these ultrasmall SNCs by conventional TEM is extremely challenging. Therefore, we attempted the use of matrix-assisted laser desorption ionization time-of-flight mass spectrometry (MALDI-TOF-MS) for further determination of the core mass of PEG_4- and PEG_{18}-thiolate-coated CdSe SNCs using a trans-2-[3-(4-tert-Butylphenyl)-2-methyl-2-propenylidene]malononitrile (DCTB) matrix. Figure 3 illustrates the MALDI-TOF-MS spectra of three different chain length PEG-thiolate-coated CdSe SNCs. The peak at m/z 6505, evident in all of the samples, corresponds to a stoichiometric $(CdSe)_{34}$ core. In contrast, the energy dispersive X-ray spectroscopy (EDS) analysis of PEG_4-thiolate-coated CdSe SNCs confirmed the Cd:Se ratio of 1.33:1.0 (Figure S1), which is consistent with the value of 1.35:1.0 as reported for PEG_6-thiolate-coated CdSe SNCs.[42] Therefore, we assume that the overall compositions of the CdSe SNCs coated with different PEG_n-thiolates were nearly identical. Thiolate is an X-type ligand and therefore, to maintain the overall charge neutrality of the thiolate-ligand-coated SNCs, the stoichiometrically inorganic core [e.g., $(CdSe)_{34}$] should be passivated with $Cd(S\text{-}PEG)_2$, which can be referred as a Z-type ligand that attaches to the surface Se ions.[50] Thus, PEG-thiolate-ligand coated CdSe SNCs are expected to be Cd rich. Unfortunately, in the MALDI-TOF-MS analysis we were unable to determine the complete mass of the PEG_n-thiolate-coated CdSe SNCs because of the detachment of the $Cd(S\text{-}PEG)_2$ from the $(CdSe)_{34}$ core. This type of ligand detachment has been observed for thiolate-ligand-protected metal nanoparticles and SNCs during MALDI-TOF-MS analysis.[51, 52] Nevertheless, both structural and compositional analyses suggest that the size and composition of the inorganic core in PEG_n-thiolate-coated CdSe SNCs (n = 4 -150) were identical and therefore blue-shifting of the excitonic peak from n = 4 to 150 cannot be attributed to change in core size.

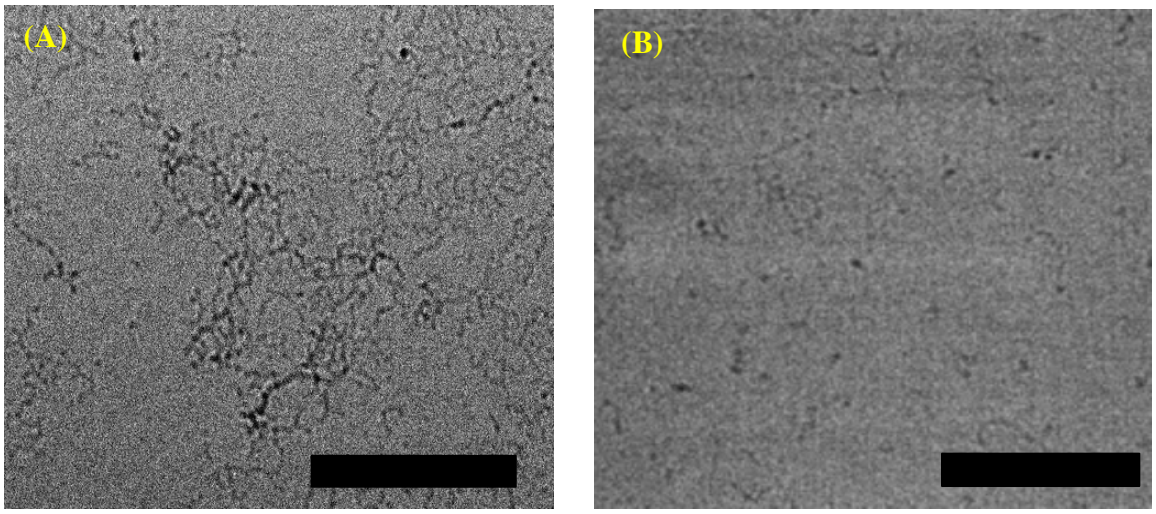

Fig. 4 Cryo-TEM images of PEG_4- (A) and PEG_{150}- (B) thiolate-coated CdSe SNCs. The aqueous solution of SNCs was frozen by liquid nitrogen inside the cell. The dark black dots are the CdSe SNCs. The images were taken at 200 kV operating voltage. Scale bars are 20 nm.

Though our conventional TEM analysis strongly supports electronic coupling of PEG_4- or PEG_{150}-thiolate-coated CdSe SNCs in solution due to their spatial organization, this analysis is inadequate to determine existence of ordered assembly in solution. We performed Cryo-TEM of PEG_4- and PEG_{150}-thiolate-coated CdSe SNCs as shown in Fig. 4. The micrograph showed the appearance of pearl-necklace type assemblies of CdSe SNCs, which are coated with PEG_4-thiolate. An average 0.6 nm inter-SNC spacing was observed in pearl-necklace assembly. This spacing is shorter than twice the length of fully stretched PEG_4-thiols (1.0 nm) but corresponds reasonably well to the expected radius of gyration for PEG polymers in an appropriate solvent.[39] Therefore it is reasonable to propose that SNCs were present in close proximity and this induced strong electronic coupling. At present we are not sure about the driving force responsible for pearl-necklace assemblies in solution but this could originate due to the van der Waals forces and dipole-dipole attraction between SNC cores, as observed for thioglycolic acid-capped colloidal CdTe SNCs.[53] The freshly prepared (Fig. 4) and a month old (Figure S2) sample of PEG_4-

thiolate-coated CdSe SNCs showed a similar pearl-necklace assembly without appearance of any anisotropic structures. Therefore, the PEG layer on the SNC surface acted as a diffusion barrier for additional fusion of SNCs inside the chain into nanowires as reported in the literature.[53] In contrast, PEG_{150}-thiolate-coated SNCs appeared to be isolated which could be due to the presence of a thin glycol shell around the SNCs that kept them separated. The pearl-necklace assemblies were stable in solution as no precipitation was observed after storing the solution for a month. We believe this excellent stability of the self-assembled structure could be due to the ultrasmall size of the inorganic core and high solubility character of the organic surface ligand, which drives the overall stability of the PEG_4-thiolate-coated CdSe SNCs.

Besides electronic coupling and exciton delocalization inducing the red-shift of the band-gap exciton peak, an increase in the dielectric constant of the surrounding media could also influence the exciton peak energy (bathochromic shift).[54] Therefore for quantitative determination of the coupling energy, we must consider the contribution of dielectric constant with a suitable model,[54] which is not within the scope of this article. However, for a qualitative estimation, absorption spectra of dissolved PEG_6-thiolate-coated CdSe SNCs were collected in three different solvents with varying dielectric constant (ε), dichloromethane (ε = 8.93), ethanol (ε = 24.5), and acetonitrile (ε = 37.5), as shown in Figure S3. Importantly, no noticeable change in the peak position was observed. Moreover, a PEG_{150} ligand layer would impose a higher dielectric constant compared to a PEG_4 ligand layer and under such circumstances we would expect *lower* energy first exciton peak for PEG_{150}-thiolate-coated CdSe SNCs than PEG_4-thiolate-coated SNCs, however we observed an opposite spectral response (Fig. 1A). Together our experimental data suggest that the dielectric constant has negligible effects on the red-shifts observed for different chain length PEG_n-thiolate-coated CdSe SNCs.

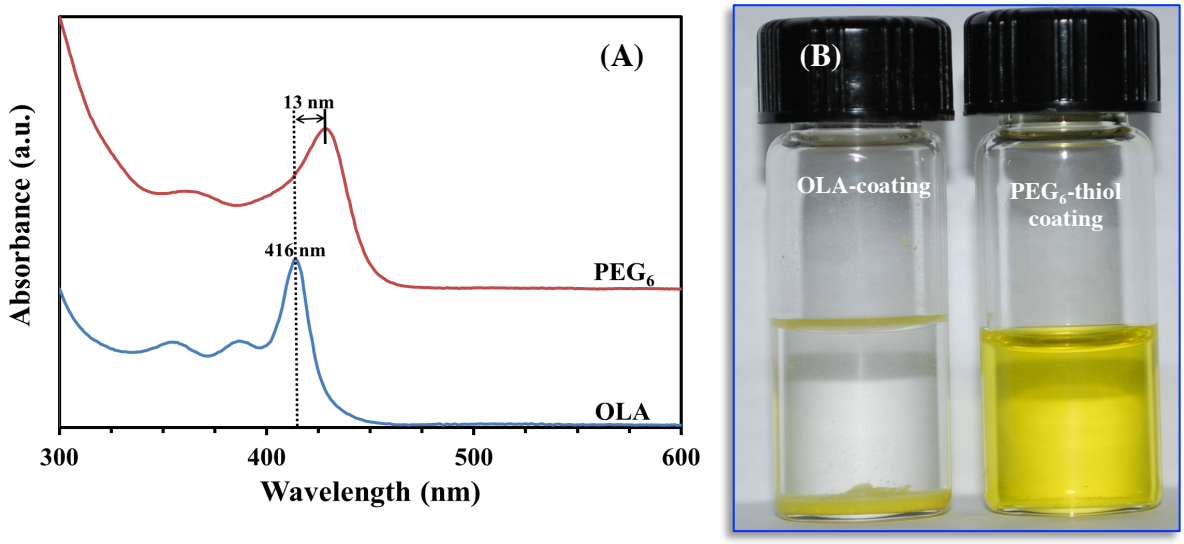

Fig. 5 (A) UV-visible absorption spectra of OLA-coated 1.6 nm diameter $(CdSe)_{34}$ SNCs (blue) and after ligand exchange reaction with PEG_6-thiols (red). An ~13 nm (90 meV) red shift of the first exciton peak was predominantly due to the increase in the electronic coupling. (B) Variable solubility properties of undissolved OLA-coated CdSe SNCs and dissolved PEG_6-thiol-coated CdSe SNCs in acetonitrile.

We performed additional experiments to further test our hypothesis that the small hydrodynamic radii and solvent-like properties of the PEG chain facilitate the inter-SNC electronic coupling. We have observed that PEG_6-thiolate-coated CdSe SNCs displayed excellent solution stability and therefore all our remaining investigation is focused on CdSe SNCs that were coated with either PEG_6-thiol or thiolate. Recently,[43] we have reported a synthesis method producing single-sized (1.6 nm in diameter) $(CdSe)_{34}$ SNCs, which were coated with oleylamine (OLA). The long hydrocarbon chain of OLA is insulating in nature, thus no electronic coupling is expected to take place in solution. However, if OLA from SNC surface can be replaced by PEG_6-thiols, the spacing between SNC will decrease and the solvent-like properties of PEG_6 chain should facilitate electronic coupling. The coupling phenomena can be studied by monitoring the band-edge excitonic peak position using UV-vis absorption spectroscopy, as demonstrated previously in Fig. 1. The synthesis of OLA-coated 1.6 nm CdSe

SNCs, solution phase ligand exchange reaction with PEG_6-thiols, and purification procedure are provided in the experimental section.

Fig. 5A illustrates the UV-vis absorption spectra of OLA- and PEG_6-thiol-coated 1.6 nm CdSe SNCs. OLA-coated CdSe SNCs displayed a band-edge excitonic peak at 416 nm (2.98 eV), which was 13 nm red-shifted to 429 nm (2.89 eV) upon ligand exchange. An ~90 meV change in the exciton peak energy is feasible when the SNCs participate in electronic coupling, but first it must be confirmed that the ligand exchange procedure was successful and the PEG_6-thiols successfully replaced the OLA ligands, and the change is not simply due to changes of the local dielectric environment caused by the ligand exchange reaction. First, OLA-coated CdSe SNCs are not soluble in acetonitrile whereas after ligand exchange reaction the CdSe SNCs were completely soluble in acetonitrile, suggesting attachment of PEG-thiol to CdSe SNC core surface (Fig. 5B). We have previously demonstrated the unique solubility properties of PEG_6-thiolate-coated CdSe SNCs (Figure S3).[42] Second, the ^{1}H NMR analysis of the purified PEG_6-thiols exchange product indeed confirmed that ~95% of the surface was coated with PEG_6-thiols with some residual OLA present (Figure S4). Third, the broadness of the peaks associated to PEG_6-thiols and presence of H-S- proton at ~2.0 ppm suggest that the PEG_6-thiol was attached to the $(CdSe)_{34}$ SNCs surface as a neutral two electron donor ligand like OLA. Finally, our MALDI-TOF-MS analysis of both OLA- and PEG_6-thiol-coated CdSe SNCs showed similar core mass (Figure S5). This is important in the context of ligand exchange reaction, which could induce the change in the core composition resulting in red-shifting of the band-edge excitonic peak position. Attachment of PEG_6-thiol as a neutral ligand onto the stoichiometric $(CdSe)_{34}$ core also supports the overall charge neutrality of the ligand-coated SNCs.

It is important to mention that the directly synthesized PEG_6-thiol-coated $(CdSe)_{34}$ SNCs surface contained a Z-type ligand, $Cd(S\text{-}PEG)_2$, whereas PEG_6-thiol was attached to the OLA-coated $(CdSe)_{34}$ SNCs surface as a L-type ligand after the ligand exchange reaction.[50] Though the $(CdSe)_{34}$ SNCs surface contained different ligand environment, they displayed a nearly identical excitonic band-gap of ~429 nm. The Se^{2-} sites in $(CdSe)_{34}$ SNCs have available electron density to donate to a σ or π-accepting ligand, where $Cd(S\text{-}PEG)_2$ is a σ-accepting ligand. Thus, the wave functions of the photogenerated electrons could delocalize into the ligand orbitals and reduce the excitonic band-gap by red-shifting to a higher wavelength, which was not observed. Therefore, we can rule out the possibility of electron delocalization in the case of $Cd(S\text{-}PEG)_2$-coated $(CdSe)_{34}$ SNCs. According to previous reports,[5, 55] both correct symmetry matching and energy level alignment between $(CdSe)_{34}$ SNCs and $Cd(S\text{-}PEG)_2$ orbitals are necessary to form hybrid interfacial orbitals to facilitate the wave function expansion into the ligand monolayer. We believe such an electronic interaction did not occur for $Cd(S\text{-}PEG)_2$-coated $(CdSe)_{34}$ SNCs, which could be due to either incorrect symmetry matching and/or poor energy alignment.

We also performed photoluminescence (PL) measurements of the PEG_6-thiol ligand exchange product to confirm our hypothesis that the CdSe SNCs surface was coated with two electrons donor neutral thiols ($H\text{-}S\text{-}PEG_6$) and not anionic thiolates ($-S\text{-}PEG_6$). The exchange product showed no change in the band-edge PL intensity as compared to OLA-coated CdSe SNCs (data not shown). Since our exchange reaction was conducted in organic solvent, therefore we would expect that thiol remains protonated and attaches onto CdSe SNCs surface as a neutral ligand rather an anionic ligand. The attachment of thiolate to surface Cd sites should lead to quenching of PL because of the formation of hole traps that prevent radiative recombination of excitons, but this is not observed in the present investigation. All of the above data support the

hypothesis that the addition of PEG_6-thiols to an organic solvent solution of OLA-coated CdSe SNCs resulted in PEG_6-thiol-coated SNCs. The solvent-like properties of PEG lead to strong inter-SNC electronic coupling and display ~90 meV change in the exciton peak energy.

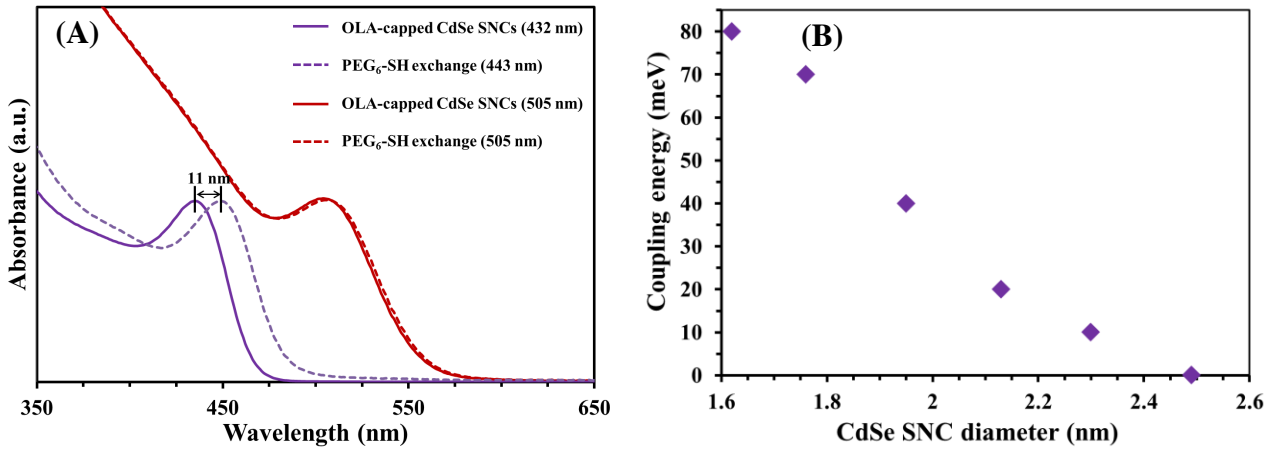

Fig. 6 (A) UV-visible absorption spectra of OLA-coated 1.8 (purple) and 2.5 nm (red) diameter CdSe SNCs before and after ligand exchange reaction with PEG_6-thiols. An ~11 nm (70 meV) red shift of the first exciton peak for 1.8 nm CdSe SNCs suggested electronic coupling where as such interaction was nearly negligible for 2.5 nm SNCs. (B) Experimentally determined coupling energy as a function of SNC diameter. The coupling energy was measured from UV-visible absorption spectra (Figure 5A and 6A) whereas diameter was calculated from an empirical sizing equation.

Size Dependent Excitonic Coupling Energy. Previous literature reports on size dependent electronic coupling studies demonstrated that the coupling strength increased with decreased SNC size.[33, 37, 56] Based on this experimental observation, SNCs having <2.5 nm in diameter and coated with suitable surface passivating ligands are expected to display strong electronic coupling in solution. To investigate size dependent electronic coupling, OLA-coated 1.8 nm to 2.5 nm CdSe SNCs were synthesized according to the procedure described for 1.6 nm SNCs with slight modification (see experimental section). Ligand exchange reactions were performed in solution to replace original insulating OLA ligands with PEG_6-thiol to reduce the inter-SNC distance and increase the electronic coupling. Fig. 6A illustrates the UV-visible absorption

spectra of 1.8 and 2.5 nm CdSe SNCs before and after PEG_6-thiol exchange. In the case of the largest CdSe SNC size (2.5 nm in diameter) no noticeable change in the peak position was observed whereas 1.8 and 2.3 nm diameter SNCs displayed 70 and 10 meV coupling energy, respectively (Fig. 6B).

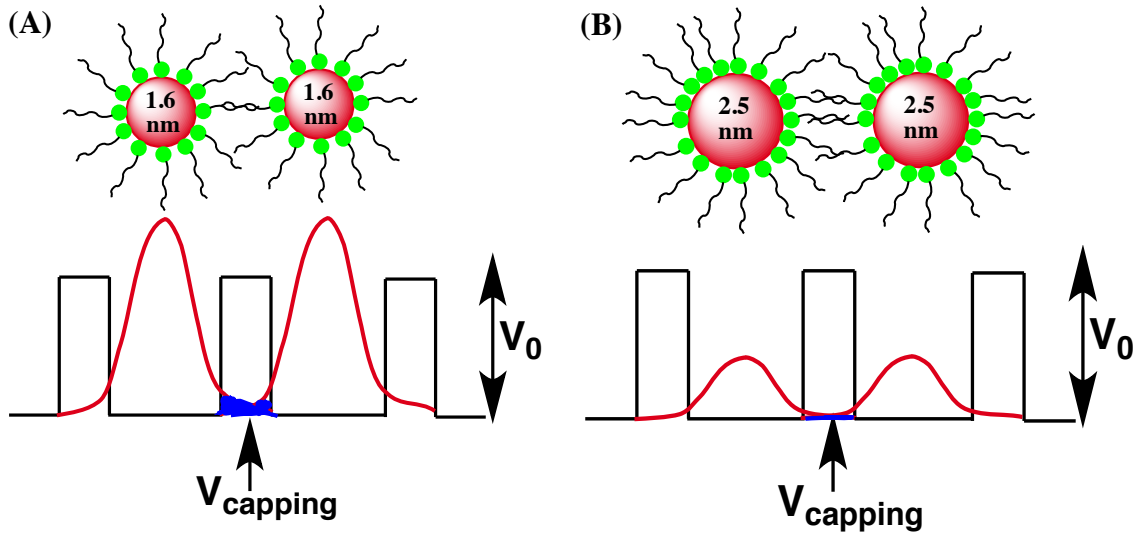

Fig. 7 Schematic illustration of the plots of the electron wave functions in two adjacent SNCs separated by $V_{capping}$ = 1.0 nm. The blue shading represents overlap of exciton wave functions, which will be higher for smaller SNCs (A) and smaller overlap for larger SNCs (B). Therefore stronger electronic coupling and higher coupling energy will be observed for smaller CdSe SNCs. The image is not to scale.

According to the mathematic model proposed by Efros and coworkers, the carrier mobility of a SNC solid increases with decreasing SNC size.[57] The mobility of the charge carrier is directly related to the electronic coupling between neighboring SNCs where higher coupling would result in faster mobility. In the case of smaller SNCs, the kinetic energy of the exciton (either electron or hole) is higher than the columbic interaction energy of an electron-hole pair.[47, 48] Therefore, for smaller SNCs (e.g., 1.6 nm diameter CdSe SNC), the exciton wave functions could easily fill the inorganic core volume and leak outside the core boundary compared to larger SNCs (e.g., 2.5 nm diameter CdSe SNC). A strong electronic coupling is expected to happen

when a large fraction of exciton wave functions expand beyond the core boundary, overlap, and entangle with wave functions from adjacent SNCs, as illustrated in Fig. 7. The exciton wave functions for 1.6 and 2.3 nm CdSe SNCs are shown where the thickness of the potential barrier ($V_{capping}$) due to PEG_6-thiolate layer is 1.2 nm (hydrodynamic radii of PEG_6 chain is 0.6 nm)[39] and the barrier height is V_0. Taken together, previous theoretical work strongly supports our experimental data that stronger electronic coupling would be observed for smaller size SNCs. To more quantitatively determine the size dependent electronic coupling energy further theoretical calculation is required and currently under our investigation.

Electronic Coupling of CdSe SNC Thin-Films. The ability to display strong electronic coupling of colloidal SNCs has been utilized to design optoelectronic devices. In this context, a solid support is required to assemble the colloidal SNCs in well-ordered thin-films where strong electronic coupling will remain active. In this article, we have already demonstrated dissolved PEG_n-thiolate-coated CdSe SNCs in solution displayed electronic coupling because of their pearl-necklace type assembly. In this section, we explore the electronic coupling of PEG_n-thiolate-coated CdSe SNCs spin-cast as thin-films (200 nm in thickens) onto glass supports. In our first investigation, the electronic coupling was studied as a function of annealing temperature using PEG_6-thiolate-coated CdSe SNCs. Even though CdSe SNCs coated with PEG_4-thiolate displayed the highest electronic coupling, the low boiling point (~150 ^oC)[41] of the ligand could volatilize during high temperature annealing, and distort the film morphology including cracking, and also create multiple trap states.[29] To avoid these undesirable structural and electronic changes, we used CdSe SNCs coated with PEG_6-thiolate, which has a higher boiling point (~250 ^oC).

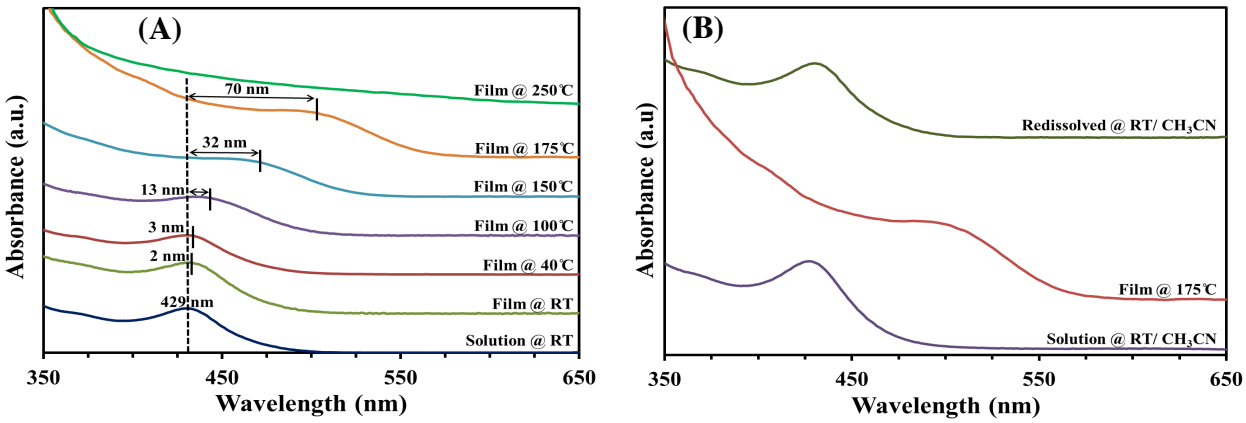

Fig. 8 (A) UV-visible absorption spectra of PEG_6-thiolate-coated 1.6 nm CdSe SNC films on glass substrates as a function of annealing temperature. (B) UV-visible absorption spectra of PEG_6-thiolate-coated 1.6 nm CdSe SNCs at different physiological conditions: Dissolved SNCs in CH_3CN before film preparation at room temperature (purple), thin-film on glass substrate annealed at 175 ºC (red), and redissolved film in CH_3CN at room temperature (green).

Fig. 8A illustrates the temperature dependent absorption spectra of CdSe SNC thin-films. Annealing the film caused red-shifting of the band-edge excitonic peak. An ~13 nm red-shift was detected at 100 ^{o}C annealing temperature. The change is dramatic as the temperature was raised to 175 ^{o}C where ~70 nm (400 meV) shift observed along with broadening of the band-edge excitonic peak. The broadness of the peak was due to the electronic coupling as reported previously.[33, 35, 37] Increasing the annealing temperature likely caused the trapped solvent molecules inside the film to evaporate and the film to become more compact, leading to decreased inter-SNC spacing and the formation of close-packed solids of CdSe SNCs ("superlattices"). Importantly, the solution phase absorption property of the CdSe SNCs can be regained when the film was redissolved in CH_3CN by sonicating the 175 ^{o}C-annealed film (Fig. 8B). The PEG chains collapse in the dry films, but SNCs maintained their structural integrity. Based on this observation, we overruled the possibility of PEG_6-thiolate desorption from the SNC surface that may influence the inter-SNC interaction as demonstrated before for small

molecule or ion coated SNCs.[18, 19, 22, 25, 28-30, 32, 36] In contrast, 100 °C annealed film of OLA-coated CdSe SNCs did not display any electronic coupling (Figure S6). This experimental result confirms that the long chain aliphatic amines (e.g., OLA) are insulating in nature and do not allow wave functions of neighboring SNC to couple and form an extended delocalize state.

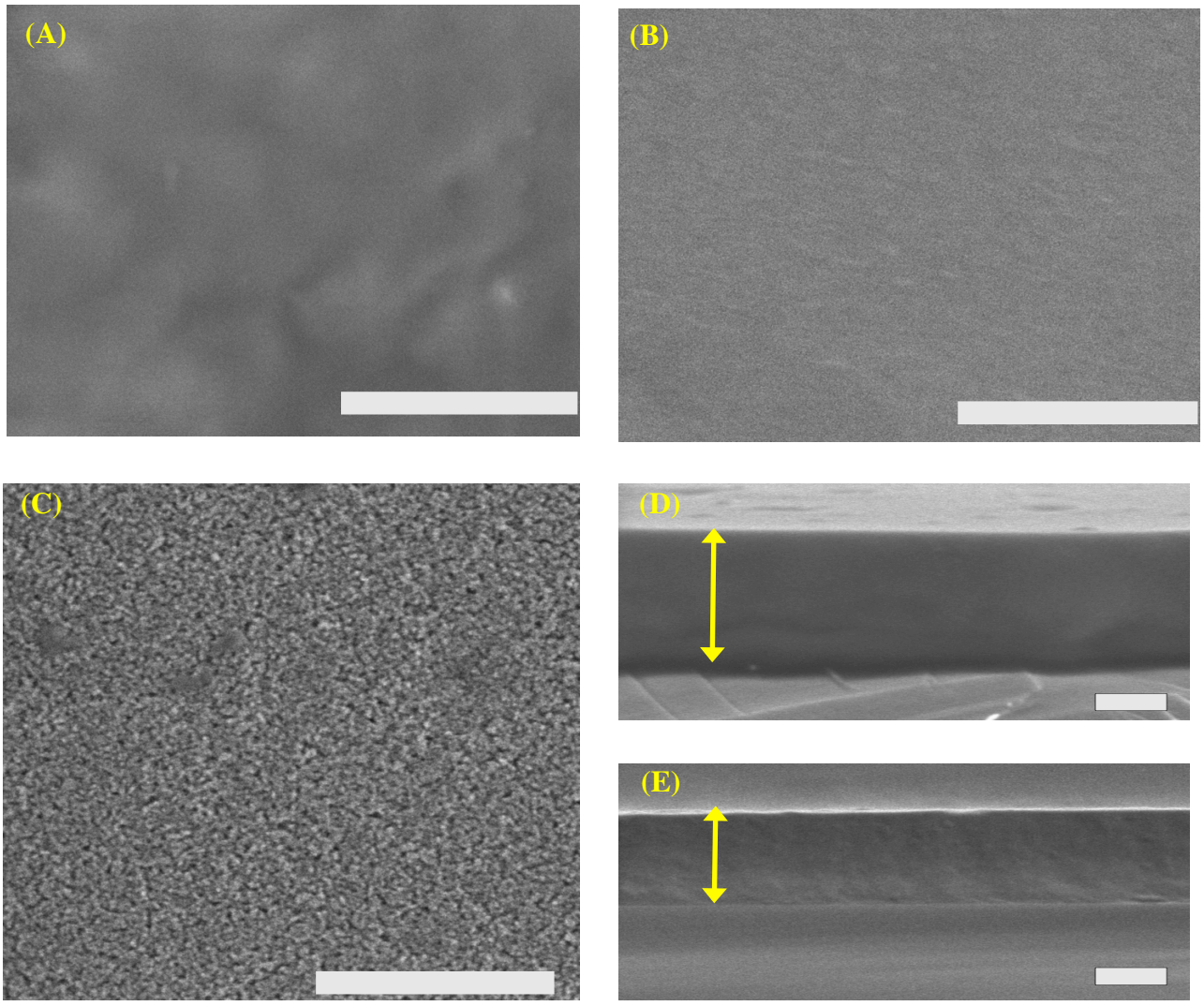

Fig. 9 SEM images of PEG_6-thiolate-coated 1.6 nm CdSe SNC films as a function of annealing temperature. (A) As prepared film at room temperature, (B) annealing at 175 °C, and (C) annealing at 250 °C. Scale bars are 500 nm. The thickness (double headed arrow) of SNC films at (D) room temperature and (E) after annealing at 175 °C. The scale bars are 100 nm.

Annealing the film >200 ^{o}C resulted in the complete disappearance of the band-edge excitonic peak features as similar to bulk CdSe. We believe at higher temperature a permanent structural change occurred where PEG_6-thiolates completely detached from CdSe SNC surface and these ultrasmall SNCs were fused together to form a bulk structure. Therefore, red-shifting and broadening of the excitonic peak <175 ^{o}C was a result of strong electronic coupling between SNCs and was not due to any structural changes. Better ordering of SNCs and a lower potential barrier are critical for stronger quantum mechanical coupling. Additionally we would expect the formation of delocalized and extended states (minibands) in strongly coupled SNCs as similar to one-dimensional superlattice of quantum wells.[58]

The SEM analysis (Fig. 9) of PEG_6-thiolate-coated 1.6 nm CdSe SNCs films after temperature treatment (175 ^{o}C) showed no apparent change in the morphology compared to as prepared films at room temperature. Interestingly, the films were smooth and crack free, similar to structural features that are generally observed in *charged* polymeric thin-films.[59] We also observed that film thickness decreases with heat treatment. The 250 ^{o}C annealed film showed small grain growth. We used the SAXS technique to investigate structural changes such as ordering and average inter-SNC spacing of the PEG_6-thiolate-coated 1.6 nm CdSe SNC films as a function of annealing temperature. Fig. 10A shows the SAXS profile as a function of annealing temperature. Interestingly, the SAXS peak (Fig. 10B) becomes narrower as the temperature was increased, which suggests that there was either an increase of SNC size or

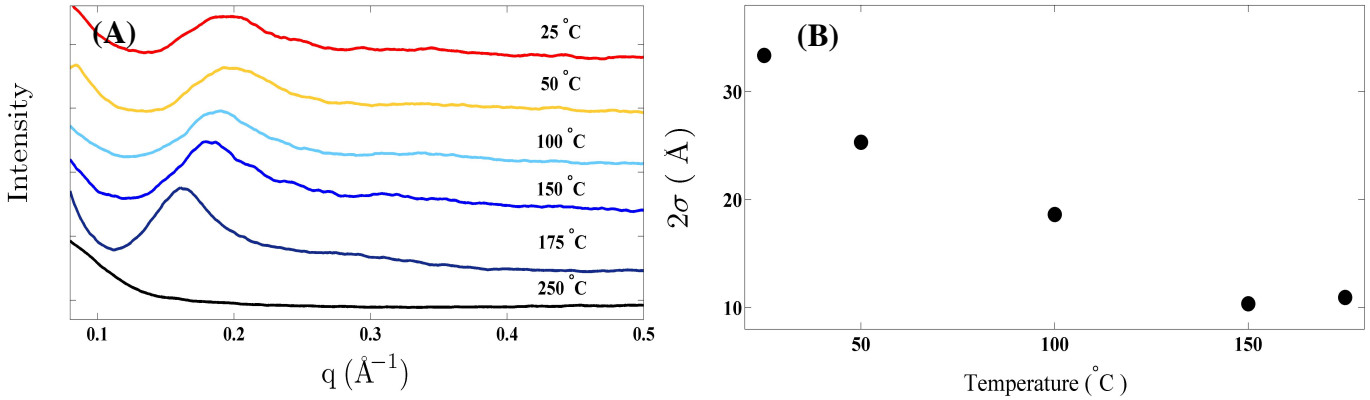

Fig. 10 (A) SAXS patterns of PEG_6-thiolate-coated 1.6 nm CdSe SNC films as a function of annealing temperature. (B) Relation between SAXS peak width with annealing temperature.

higher ordering of SNCs inside the film.[60] We hypothesize that no change in SNC size took place because the 175 °C annealed film retained the excitonic band-gap property of 1.6 CdSe SNCs after redissolving in solvent (see Fig. 8B). The SEM analysis (Fig. 9) clearly showed decreased film thickness, therefore we believe that evaporation of trapped solvent inside the film and collapse of the PEG chain, together densify the films and increase the short-range ordering of SNCs inside the film. Additionally, with increased annealing temperature, the PEG chain could form some ordered structure that would result in an ordered array or periodic SNCs.[61] At 250 °C annealing temperature, the SAXS peak completely disappeared, which could be due to melting and desorption of the PEG-thiolate ligand from the surface of the CdSe SNCs that resulting in degradation of SNCs.

The strong electronic coupling between PEG-thiolate-coated CdSe SNCs in their solid films demonstrated here has provided several important advantages over existing SNC-based thin-film materials. First, there is no need to perform a solid phase ligand exchange reaction to replace insulating ligands, a process that typically leads to a dramatic structural rearrangement of SNCs

and results in the appearance of cracks and voids in the solid films or fusion of SNCs in such films.[19, 32] Second, we can prevent formation of trap states and recombination sites while maintaining strong electronic coupling by using nonvolatile PEG-thiolate ligands instead of using chloride,[22] thiocyanate,[25] sulfide,[26-28] metal chalcogenide complexes,[13, 29-31] tetrafluoroborate,[23, 24] hydrazine,[14, 32] or pyridine.[19] Third, SNCs coated with either small molecules or various ions are susceptible to undergoing fast oxidation even at ambient conditions[19] making processing during device fabrication very difficult. All of these drawbacks can be avoided using our ligand-coated SNCs where the thin-film was almost defect free (cracks or sintering). Most importantly, PEG_{150}-thiolate-coated CdSe SNCs displayed extraordinarily higher stability than PEG_6-thiolate-coated SNCs under harsh conditions (i.e., presence of light and air). However, PEG_6-thiolate-coated CdSe SNCs possessed higher stability than OLA-coated CdSe SNCs. The greater stability of our PEG_n-thiolate-coated CdSe SNCs is crucial for future device applications. A detailed study concerning the stability of the CdSe SNCs coated with PEG_n-thiolate under various conditions will be published elsewhere.

Conclusions

The ligand-controlled strong electronic coupling - up to 405 meV reduction of excitonic energy gap - between *solvent-like* ligand-coated CdSe SNCs in thin-films resulting from the expansion of exciton wave function beyond the boundary of the inorganic-core, hybridize and delocalize has several potential benefits: (1) The PEG-thiolate-coated CdSe SNCs possess diverse solubility character. Appropriate selection of solvent will allow the preparation of large-scale thin-films with better structural properties such as enhanced homogeneity and less void space. Thus, there is no need to use additional conductive materials to backfill the voids through atomic-layer

deposition techniques.[27] Therefore, we could eliminate energy disorder while maintaining strong electronic coupling between SNCs thus facilitating their uses in high-performance light-emitting diodes and field-effect transistor fabrication. (2) PEG chains can impart liquid crystalline characteristics to ligand-coated SNCs, which improve the SNCs packing in thin-film. Because of the strong electronic coupling between thiolate-coated SNCs, and physical and electrochemical properties of hybrid redox polyethers enable hopping-mediated faster charge transport in thin-films and therefore enhance their application in electrochromic devices. (3) Current knowledge of electrochemical properties of ligand-coated semiconductor nanocrystals is very limited because of fast decomposition during measurement[62] caused by the insulating nature of existing surface ligand coatings. However, strong inter-SNC electronic coupling in organic solvents such as CH_2Cl_2 and CH_3CN would increase the stability of PEG-thiolate-coated CdSe SNCs during the solution-phase electrochemical characterization because the extra charge can delocalize to neighboring SNCs through solvent-like ligand shell and/or be stabilized by an *"outer-sphere"* reorganization. Enhanced stability will provide quantitative information about the electrochemical oxidation and reduction potentials of ligand-coated SNCs and therefore enable the control of the generation and transfer of charge carriers, which should facilitate the design of efficient electronic materials for photovoltaic applications.

Electronic Supplementary Information. Additional experimental procedure, UV-vis absorption, EDS, and NMR spectra and cryo-TEM image.

ACKNOWLEDGEMENT

The research was partially supported by IUPUI startup funds and financial support from the Integrated Nanosystems Development Institute at IUPUI. The authors would also like to thank David Morgan (Indiana University Bloomington) for helping with Cryo-TEM analysis.

REFERENCES

1. D. A. Hines and P. V. Kamat, *ACS Applied Materials & Interfaces*, 2014, **6**, 3041-3057.
2. N. A. Anderson and T. Lian, *Annual Review of Physical Chemistry*, 2005, **56**, 491-519.
3. M. D. Peterson, L. C. Cass, R. D. Harris, K. Edme, K. Sung and E. A. Weiss, *Annual Review of Physical Chemistry*, 2014, **65**, 317-339.
4. C. Giansante, I. Infante, E. Fabiano, R. Grisorio, G. P. Suranna and G. Gigli, *Journal of the American Chemical Society*, 2015, **137**, 1875-1886.
5. M. B. Teunis, S. Dolai and R. Sardar, *Langmuir*, 2014, **30**, 7851-7858.
6. S. A. Fischer, A. M. Crotty, S. V. Kilina, S. A. Ivanov and S. Tretiak, *Nanoscale*, 2012, **4**, 904-914.
7. M. Gao, C. Lesser, S. Kirstein, H. Möhwald, A. L. Rogach and H. Weller, *Journal of Applied Physics*, 2000, **87**, 2297-2302.
8. H. Mattoussi, L. H. Radzilowski, B. O. Dabbousi, E. L. Thomas, M. G. Bawendi and M. F. Rubner, *Journal of Applied Physics*, 1998, **83**, 7965-7974.
9. S. Coe, W.-K. Woo, M. Bawendi and V. Bulovic, *Nature*, 2002, **420**, 800-803.
10. V. L. Colvin, M. C. Schlamp and A. P. Alivisatos, *Nature*, 1994, **370**, 354-357.
11. D. C. Oertel, M. G. Bawendi, A. C. Arango and V. Bulović, *Applied Physics Letters*, 2005, **87**, -.
12. G. Konstantatos, I. Howard, A. Fischer, S. Hoogland, J. Clifford, E. Klem, L. Levina and E. H. Sargent, *Nature*, 2006, **442**, 180-183.
13. M. V. Kovalenko, M. Scheele and D. V. Talapin, *Science*, 2009, **324**, 1417-1420.
14. D. V. Talapin and C. B. Murray, *Science*, 2005, **310**, 86-89.
15. K. Tvrdy, P. A. Frantsuzov and P. V. Kamat, *Proceedings of the National Academy of Sciences*, 2011, **108**, 29-34.
16. I. Gur, N. A. Fromer, M. L. Geier and A. P. Alivisatos, *Science*, 2005, **310**, 462-465.
17. C. L. Choi and A. P. Alivisatos, *Annual Review of Physical Chemistry*, 2010, **61**, 369-389.
18. J. M. Luther, M. Law, Q. Song, C. L. Perkins, M. C. Beard and A. J. Nozik, *ACS Nano*, 2008, **2**, 271-280.
19. M. Law, J. M. Luther, Q. Song, B. K. Hughes, C. L. Perkins and A. J. Nozik, *Journal of the American Chemical Society*, 2008, **130**, 5974-5985.
20. D. H. Webber and R. L. Brutchey, *Journal of the American Chemical Society*, 2011, **134**, 1085-1092.
21. D. Yu, C. Wang and P. Guyot-Sionnest, *Science*, 2003, **300**, 1277-1280.
22. Z. M. Norman, N. C. Anderson and J. S. Owen, *ACS Nano*, 2014, **8**, 7513-7521.

23. E. L. Rosen, R. Buonsanti, A. Llordes, A. M. Sawvel, D. J. Milliron and B. A. Helms, *Angewandte Chemie International Edition*, 2012, **51**, 684-689.
24. A. Dong, X. Ye, J. Chen, Y. Kang, T. Gordon, J. M. Kikkawa and C. B. Murray, *Journal of the American Chemical Society*, 2010, **133**, 998-1006.
25. A. T. Fafarman, W.-k. Koh, B. T. Diroll, D. K. Kim, D.-K. Ko, S. J. Oh, X. Ye, V. Doan-Nguyen, M. R. Crump, D. C. Reifsnyder, C. B. Murray and C. R. Kagan, *Journal of the American Chemical Society*, 2011, **133**, 15753-15761.
26. A. Nag, M. V. Kovalenko, J.-S. Lee, W. Liu, B. Spokoyny and D. V. Talapin, *Journal of the American Chemical Society*, 2011, **133**, 10612-10620.
27. Y. Liu, J. Tolentino, M. Gibbs, R. Ihly, C. L. Perkins, Y. Liu, N. Crawford, J. C. Hemminger and M. Law, *Nano Letters*, 2013, **13**, 1578-1587.
28. H. Zhang, B. Hu, L. Sun, R. Hovden, F. W. Wise, D. A. Muller and R. D. Robinson, *Nano Letters*, 2011, **11**, 5356-5361.
29. D. V. Talapin, J.-S. Lee, M. V. Kovalenko and E. V. Shevchenko, *Chemical Reviews*, 2009, **110**, 389-458.
30. R. W. Crisp, J. N. Schrauben, M. C. Beard, J. M. Luther and J. C. Johnson, *Nano Letters*, 2013, **13**, 4862-4869.
31. J.-S. Lee, M. V. Kovalenko, J. Huang, D. S. Chung and D. V. Talapin, *Nature Nanotechnology*, 2011, **6**, 348-352.
32. K. J. Williams, W. A. Tisdale, K. S. Leschkies, G. Haugstad, D. J. Norris, E. S. Aydil and X. Y. Zhu, *ACS Nano*, 2009, **3**, 1532-1538.
33. O. I. Micic, S. P. Ahrenkiel and A. J. Nozik, *Applied Physics Letters*, 2001, **78**, 4022-4024.
34. M. C. Beard, G. M. Turner, J. E. Murphy, O. I. Micic, M. C. Hanna, A. J. Nozik and C. A. Schmuttenmaer, *Nano Letters*, 2003, **3**, 1695-1699.
35. G. W. Bryant and W. Jaskolski, *Physica E: Low-dimensional Systems and Nanostructures*, 2002, **13**, 293-296.
36. J.-H. Choi, A. T. Fafarman, S. J. Oh, D.-K. Ko, D. K. Kim, B. T. Diroll, S. Muramoto, J. G. Gillen, C. B. Murray and C. R. Kagan, *Nano Letters*, 2012, **12**, 2631-2638.
37. R. Koole, P. Liljeroth, C. de Mello Donega, D. Vanmaekelbergh and A. Meijerink, *Journal of the American Chemical Society*, 2006, **128**, 10436-10441.
38. Y. Liang, J. E. Thorne and B. A. Parkinson, *Langmuir*, 2012, **28**, 11072-11077.
39. M. E. Williams, H. Masui, J. W. Long, J. Malik and R. W. Murray, *Journal of the American Chemical Society*, 1997, **119**, 1997-2005.
40. J. W. Long, I. K. Kim and R. W. Murray, *Journal of the American Chemical Society*, 1997, **119**, 11510-11515.
41. A. W. Snow and E. E. Foos, *Synthesis*, 2003, **4**, 509-512.
42. K. Lawrence, S. Dolai, Y.-H. Lin, A. Dass and R. Sardar, *RSC Advances*, 2014, **4**, 30742-30753.
43. S. Dolai, P. R. Nimmala, M. Mandal, B. B. Muhoberac, K. Dria, A. Dass and R. Sardar, *Chemistry of Materials*, 2014, **26**, 1278-1285.
44. S. Kudera, M. Zanella, C. Giannini, A. Rizzo, Y. Li, G. Gigli, R. Cingolani, G. Ciccarella, W. Spahl, W. J. Parak and L. Manna, *Advanced Materials*, 2007, **19**, 548-552.
45. A. D. Dukes, J. R. McBride and S. J. Rosenthal, *Chemistry of Materials*, 2010, **22**, 6402-6408.

46. Y. Wang, Y. Zhang, F. Wang, D. E. Giblin, J. Hoy, H. W. Rohrs, R. A. Loomis and W. E. Buhro, *Chemistry of Materials*, 2014, **26**, 2233-2243.
47. L. E. Brus, *The Journal of Chemical Physics*, 1983, **79**, 5566-5571.
48. M. T. Frederick, V. A. Amin, L. C. Cass and E. A. Weiss, *Nano Letters*, 2011, **11**, 5455-5460.
49. C. A. Leatherdale, C. R. Kagan, N. Y. Morgan, S. A. Empedocles, M. A. Kastner and M. G. Bawendi, *Physical Review B*, 2000, **62**, 2669-2680.
50. N. C. Anderson, M. P. Hendricks, J. J. Choi and J. S. Owen, *Journal of the American Chemical Society*, 2013, **135**, 18536-18548.
51. A. Dass, A. Stevenson, G. R. Dubay, J. B. Tracy and R. W. Murray, *Journal of the American Chemical Society*, 2008, **130**, 5940-5946.
52. J. J. Gaumet, G. A. Khitrov and G. F. Strouse, *Nano Letters*, 2002, **2**, 375-379.
53. Z. Tang, N. A. Kotov and M. Giersig, *Science*, 2002, **297**, 237-240.
54. C. A. Leatherdale and M. G. Bawendi, *Phys. Rev. B*, 2001, **63**, 165315-165316.
55. M. T. Frederick and E. A. Weiss, *ACS Nano*, 2010, **4**, 3195-3200.
56. M. V. Artemyev, A. I. Bibik, L. I. Gurinovich, S. V. Gaponenko and U. Woggon, *Physical Review B*, 1999, **60**, 1504-1506.
57. A. Shabaev, A. L. Efros and A. L. Efros, *Nano Letters*, 2013, **13**, 5454-5461.
58. L. Han, J. Liu, N. Yu, Z. Liu, J. Gu, J. Lu and W. Ma, *Nanoscale*, 2015, **7**, 2461-2470.
59. J. M. D'Arcy, H. D. Tran, V. C. Tung, A. K. Tucker-Schwartz, R. P. Wong, Y. Yang and R. B. Kaner, *Proceedings of the National Academy of Sciences*, 2010, **107**, 19673-19678.
60. B. Ingham, T. H. Lim, C. J. Dotzler, A. Henning, M. F. Toney and R. D. Tilley, *Chemistry of Materials*, 2011, **23**, 3312-3317.
61. E. Kim, H. Ahn, S. Park, H. Lee, M. Lee, S. Lee, T. Kim, E.-A. Kwak, J. H. Lee, X. Lei, J. Huh, J. Bang, B. Lee and D. Y. Ryu, *ACS Nano*, 2013, **7**, 1952-1960.
62. M. Amelia, C. Lincheneau, S. Silvi and A. Credi, *Chemical Society Reviews*, 2012, **41**, 5728-5743.